Radiative power and electron cooling rates for oxygen in steady-state and transient plasmas at densities beyond the coronal limit

C. Keane* and C. H. Skinner
Plasma Physics Laboratory, Princeton University, James Forrestal Campus, P.O. Box 451, Princeton, New Jersey 08544-0451
(Received 11 December 1985)

We have developed a time-dependent, collisional-radiative model to calculate radiative power and electron cooling rates for oxygen at intermediate densities ($10^{16} \leq n_e \leq 10^{20}$ cm^{-3}) where the usual coronal approximation is not valid. Large differences from coronal values are predicted. The behavior of the steady-state radiative-power-loss coefficient, L_z, is investigated as the electron density is increased. Generalized power-loss coefficients applicable to transient plasmas are derived and applied to ionizing and recombining oxygen plasmas. Time-dependent effects are found to play a large role both in terms of the total radiated power and the net electron-energy-loss rate.

I. INTRODUCTION

Radiative power losses and associated electron cooling rates from plasmas are important in many applications and are central to recent work on the development of a soft-x-ray laser based on fast radiative cooling of a confined recombining plasma. A gain-length product of 6.5 on the C VI 182-Å line was achieved at the Princeton Plasma Physics Laboratory (PPPL) in a recombining magnetically confined plasma column, with a 120% increase in stimulated emission observed in initial experiments with a soft-x-ray mirror having 12% reflectivity at 182 Å.[1] At Lawrence Livermore National Laboratory, significant amplification was obtained at 206 and 209 Å in neonlike selenium[2] with a gain-length product of 6–7. The absence of the $J=0$ to $J=1$ transition at 183 Å, predicted by a collisional excitation model[3] to have the highest gain, prompted Apruzese *et al.*[4] to postulate a controversial alternative explanation of the Livermore results based on rapid radiative cooling in a recombining plasma. In an experiment at the University of Rochester,[5] gain was reported on the C VI 182-Å transition and interpreted in terms of radiation cooling by selenium; this has been supported recently in more detailed modeling.[6]

Calculations of radiated power in the coronal regime are available[7–10] and have been widely applied to low-density plasmas. A formal generalization of the theory to include metastable levels has been published by Summers and Hooper.[11] Several studies of the radiated power from low-density, transient, ionizing plasmas have also been reported.[12–14] At higher electron densities and lower electron temperatures the coronal approximation is no longer valid and the ionization balance (fraction of ions in each charge state) and radiative cooling coefficients (radiated power per ion per electron) become density dependent and differ from the coronal values. In a series of papers, Duston and Davis[15,16] have investigated the radiative power coefficients for carbon, oxygen, and aluminum in high-density steady-state plasmas in both the optically thin and thick cases. The transient behavior of the ionization balance can also play a significant role in modifying the radiated power from its steady-state value.

This paper presents a calculation of the radiative cooling properties of oxygen in equilibrium and transiently ionizing and recombining plasmas for electron densities up to $N_e = 10^{20}$ cm^{-3}. Oxygen was chosen as it is used in a soft-x-ray laser development experiment[1] as a medium in which to generate a population inversion, as well as to provide additional radiation cooling for carbon plasmas. In addition, oxygen is present in most laboratory plasmas as an impurity and its radiative-power-loss properties are of general importance.

We have outlined the atomic model to be used in Sec. II. The free electrons are assumed to be characterized by a Maxwellian distribution with an electron temperature T_e. For generality, and since it is also difficult to generate significant xuv gain in optically thick media, we treat the case of a plasma that is optically thin to its own radiation. Section III contains results for the steady-state radiative-power-loss coefficients for oxygen in the low-, intermediate-, and high-density regimes. In Sec. IV power-loss coefficients appropriate for transient plasmas are defined and calculated. Section V applies these coefficients to transiently ionizing and recombining plasmas and examines the effects of high density and transient behavior on the radiative power losses and electron cooling.

II. ATOMIC MODEL

Our approach is to calculate the oxygen ionization balance using the collisional dielectronic recombination and ionization coefficients of Summers[17,18] and then to determine the excited-state populations in each charge state and thus the total radiated power. Summers has calculated ionization and recombination coefficients valid beyond the coronal regime that explicitly take into account finite density effects such as stepwise ionization processes and collisional suppression of dielectronic recombination. These rates are an extension of the standard collisional ra-

diative coefficients first defined by Bates, Kingston, and McWhirter.[19] We have utilized these rates to generate the oxygen ionization balance in both the steady-state and transient cases.

In the steady-state case the ionization balance is given by the solution of the set of coupled equations

$$\frac{N_z}{N_{z+1}}=\frac{\alpha_z}{S_z} . \tag{1}$$

Here N_z is the ground-state population of the ion of charge z, and S_z and α_z are the collisional dielectronic ionization and recombination rates for O^{z+}.

In the case of a transient plasma we have utilized the above rates to generate the time-dependent ionization balance from the solution of the coupled set of rate equations

$$\frac{dN_z}{dt}=-N_zN_e(S_z+\alpha_{z-1})+N_{z+1}N_e\alpha_z+N_{z-1}N_eS_{z-1} . \tag{2}$$

Here N_e is the electron density. Calculation of the excited-state populations of a given charge state requires a knowledge of its energy-level structure as well as rate coefficients for all collisional and radiative processes connecting these levels. For given ground-level populations, N_z and N_{z+1}, the solution for the excited-state populations, **N**, of the ion N_z may be written in matrix notation as

$$\mathbf{N}=N_z\vec{\mathbf{Q}}^{-1}\cdot\mathbf{S}+N_{z+1}\vec{\mathbf{Q}}^{-1}\cdot\mathbf{R} . \tag{3}$$

Here **R** and **S** are column vectors which represent recombination (both three-body and radiative) to each level and excitation from the ground to each level, respectively. $\vec{\mathbf{Q}}$ is the matrix linking the excited levels through collisional and radiative processes. Q_{mk} is the rate coefficient for k-m transitions, and $-Q_{kk}$ is the total depopulation rate of level k.

The processes of collisional excitation and deexcitation, three-body recombination and collisional ionization, spontaneous radiative decay, and radiative recombination are included in the rate equations for the excited-state population model. Excited states with principal quantum number $n \leq 10$ are considered. Individual angular momentum states through principal quantum number 4 are treated separately for O^{4+}, O^{5+}, and O^{6+}. For O^{4+} and O^{6+} both the singlet and triplet spin systems have been taken into account. These systems are linked through collisions between levels of the same principal quantum number.

For O^{0+}–O^{3+} we have used a less detailed excited-state structure and made the approximation of neglecting direct contributions to excited-state populations due to recombination. For these charge states we include all of the strongly radiating, low-lying levels that dominate the steady-state radiative power losses. This simpler model, similar to that described by Suckewer,[20] was adopted for O^{0+}–O^{3+} because these charge states are peripheral to our application, and their relatively complex structure makes the development of a full model a lengthy affair. In addition, based on a comparison of a similar model to our full model for O^{4+}–O^{7+} described below, we expect this less-detailed model to be valid for O^{0+}–O^{3+} for the cases of interest in this paper. More specifically, the simpler model should be valid for most situations except for cases of strong recombination of O^{0+}–O^{4+}; we will not deal with such situations in this work.

The atomic data used in the solution of the coupled rate equations for the excited states of O^{4+}–O^{7+} were drawn from a variety of sources. Energy levels were taken from the work of Wiese[21] and Bashkin and Stoner;[22] oscillator strengths were taken from the work of Kelly[23] and Wiese.[21] For transitions not tabulated in the above sources, a Bates-Daamgard[24] calculation was used to generate the necessary data. The collisional dielectronic ionization and recombination rates used are those of Summers.[17] For collisional ionization directly out of the ground state, the rates of Bell[25] are employed, while for ionization out of excited states, the rates of Vriens and Smeets[26] are used. The sources used for dipole-allowed electron collisional excitation rates, in order of charge state, are, for O^{7+}, Clark, Sampson, and Goett[27] and Sampson;[28] for O^{6+}, Pradhan;[29] for O^{5+}, Cochrane and McWhirter;[30] and for O^{4+}, Itikawa.[31] For collisional excitation out of the ground state of the above ions into high-lying levels with $n > 3$, the hydrogenic rates of Sampson[28] were utilized when other data were not available. The rate coefficient of Seaton[32] was used for collisional excitation between excited states not covered by the sources above. For angular momentum quantum number changing collisions with $n \leq 4$ and $\Delta n = 0$, the results of Pengelly and Seaton[33] were adopted. Transitions with a change of spin originating from the ground state and terminating on levels with $n \leq 2$ were included by using the results of Itikawa[31] and Pradhan.[29] For transitions with a change of spin between excited levels, only transitions in which the principal quantum does not change are considered. For $n \leq 3$ the results of Sampson[34] are adopted and scaled[35] by n^4 for $n > 3$. Radiative recombination rates were taken from Seaton.[36] Rate coefficients for the inverse processes of collisional deexcitation and three-body recombination were obtained from detailed balance relations. Continuum radiation in the form of bremsstrahlung and radiative recombination was included, with the Gaunt factors of Karzas and Latter[37] being employed for the former.

For O^{1+}–O^{3+} the ionization and recombination rates of Summers are used to calculate the ionization balance. Here the formulation of Seaton[32] for collisional excitation out of the ground state was used, with Gaunt factors taken from the work of Post *et al.*[9] For O^{2+} the results of Eissner and Seaton[38] were used for transitions between the ground and metastable levels.

In steady state N_z and N_{z+1} are computed from Eq. (1) and the excited-state populations calculated from Eq. (3). For the transient case, Eq. (3) assumes the excited levels are in "quasi-steady-state" with the ion populations N_z and N_{z+1}. For the nonequilibrium plasmas considered in this paper, where T_e and N_e change on the time scales slower than 10^{-9} sec, this assumption is valid for all excited levels except those that decay to the ground state primarily by collisions or those that are metastable. Typical examples of levels exhibiting this behavior are the

$1s^2 2s\,2p\,{}^1P$ and ${}^3P$ levels in O^{4+}, the $1s^2 2p\,{}^2P$ level in O^{5+}, and the $1s^2 2s\,{}^3S$ and $1s^2 2p\,{}^3P$ levels in O^{6+}.

The handling of the metastable levels (and the triplet spin system in general) in O V and O VII is problematic, primarily because these metastable levels are not included in the calculations performed by Summers of the collisional dielectronic ionization and recombination coefficients. Recently,[11] Summers has outlined a method for the inclusion of these levels, although the correspondingly modified ionization and recombination rates are not yet available.

Our approach has been to treat the metastable contribution in the following way. We have included the triplet series of both O^{4+} and O^{6+} in our detailed collisional-radiative model. For a given total O^{4+} or O^{6+} population obtained from the steady-state or transient ionization balance calculation, we have iterated the solution of the coupled rate equations for the ground, metastable, and excited states until the total density in these excited states as well as the ground state equaled the total charge state density received from the ionization balance calculation. This method has the advantage of progressing smoothly from the zero-density limit (where metastable populations are negligible) to higher densities where metastable levels are typically more populated than the true ground state. A similar procedure was adopted for the $2p\,{}^1P$ level of O^{4+} and the $2p\,{}^2P$ level of O^{5+}, since at high densities these levels can have populations of the same order as the ground or nearby metastable states. In Sec. IV, we estimate the effect of including metastable levels by comparing the transient power-loss coefficients for O^{4+} and O^{6+} computed with and without the triplet spin system.

The model described above for O^{0+}–O^{7+} was checked by comparing our results for the radiated power per electron per ion L_z in the low-density limit to the coronal equilibrium results of Post *et al.*[9] The agreement is good (within a factor of 2–3) considering that both a different atomic model and different excitation rates were employed. In Sec. IV a consistency test of our model with the ionization and recombination rates of Summers is described which serves as a further test of our assumed atomic data and rate coefficient information.

III. STEADY-STATE RESULTS

Power loss from steady-state plasmas is normally presented in terms of the quantity L_z, which is the radiated power per electron per ion. The total radiated power per cm^{-3} due to a density N_T of oxygen atoms at a given T_e and N_e in steady state is

$$P_{\text{tot}} = N_T N_e L_z(N_e, T_e) \,. \tag{4}$$

In the coronal limit the radiative-power-loss function L_z is independent of electron density, and primarily represents the sum of excitation energies times the corresponding collisional excitation rates out of each ground state, weighted by the equilibrium ionization fraction of that charge state.

Figure 1 shows the steady-state radiative-power-loss coefficient L_z at $N_e = 10^{10}$, 10^{16}, 10^{17}, and 10^{18} cm^{-3}. The coronal results of Post *et al.* are also shown for comparison. The overall shape of the curve, with a peak due to L-shell radiation at low temperatures and a second peak due to K-shell radiation at high temperatures, is preserved at high density. In fact, the K-shell peak is little changed as the coronal approximation at high temperatures is still relatively good for He-like and H-like oxygen. Below 100 eV, however, significant differences emerge. First, collisional deexcitation begins to compete with radiative decay and reduces the power-loss coefficient from its coronal value. Another way to view this is that in the collisional limit the ratio of excited- to ground-state population depends only on the electron temperature, so that the cooling rate per electron per ion decreases monotonically with increasing electron density. The onset of collisional deexcitation also results in changes in the composition of the total line radiated power as the electron density is increased. This is demonstrated in Fig. 2, which shows the fraction of line radiation arising from $\Delta n \geq 1$ transitions at $N_e = 10^{10}$ and 10^{18} cm^{-3}. At $N_e = 10^{10}$ cm^{-3}, 95% of the radiation near $T_e = 20$ eV arises due to $\Delta n = 0$ transitions. At $N_e = 10^{18}$ cm^{-3}, however, $\Delta n = 0$ contributions represent only 20% of the line radiated power, since these transitions have been quenched by collisional deexcitation.

The second high-density effect on the radiative-power-loss function is the alteration of the steady-state ionization balance. As the electron density is increased, the ionization rate for a given charge state increases due to stepwise effects, while the recombination rate generally decreases due to collisional interruption of dielectronic

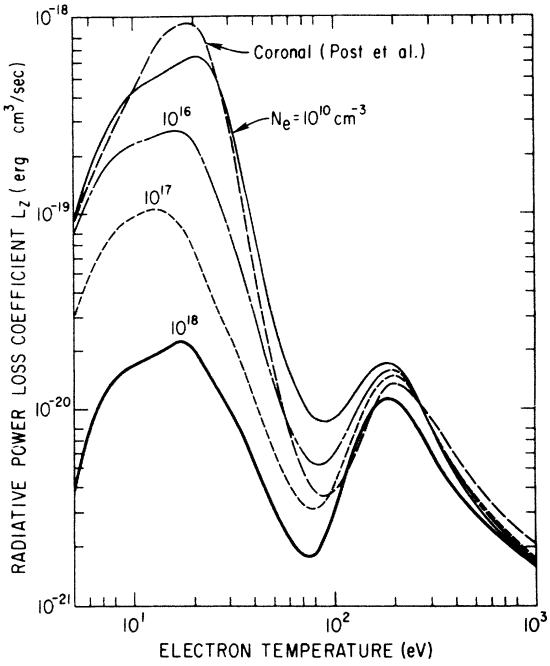

FIG. 1. Steady-state radiative-power-loss coefficient for oxygen as a function of electron temperature at several electron densities. The results at $N_e = 10^{10}$ cm^{-3} are in good agreement with the average-ion coronal model of Post *et al.*

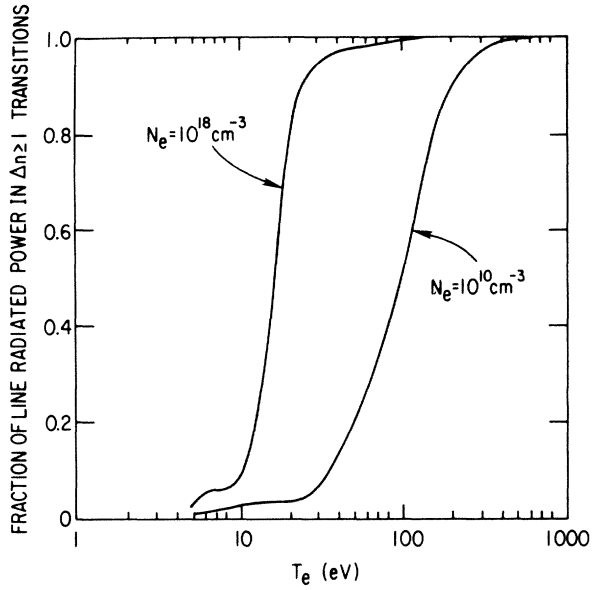

FIG. 2. Fraction of total line radiated power in $\Delta n \geq 1$ transitions for $N_e = 10^{10}$ and 10^{18} cm^{-3}.

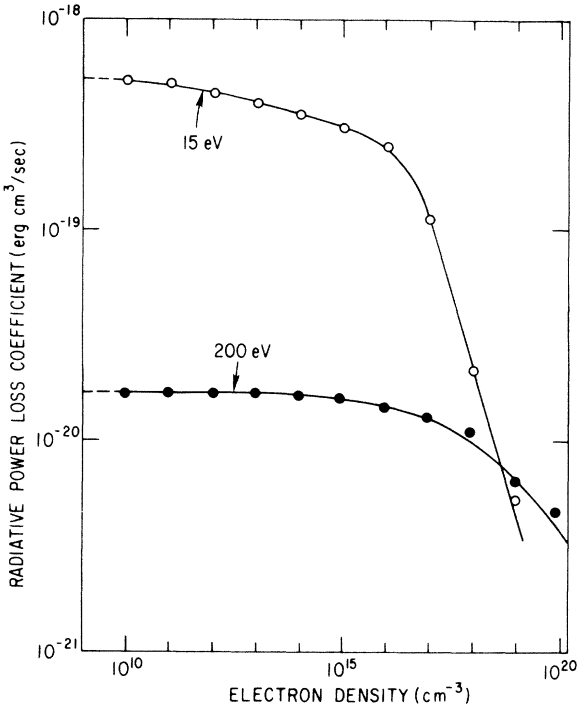

FIG. 3. Steady-state radiative-power-loss coefficient as a function of electron density at electron temperatures of 15 and 200 eV.

recombination. Both of these tend to increase the state of ionization of the plasma. The combined effect of the change in ionization balance and, more importantly, the onset of collisional deexcitation, is to reduce the radiative-power-loss coefficient at a given temperature. The steady-state results presented above include the effects of metastable levels; the deviation from the curves shown in Fig. 1 when spin systems terminating on metastable levels are not considered is typically 30% and at most a factor of 2.

Figures 3 and 4 show L_z and the average charge $\bar{Z}$ versus electron density N_e for the two electron temperatures corresponding to the K- and L-shell emission peaks in the coronal L_z curve. At 15 eV, L_z decreases slowly with density at first, due to the effect of the changing steady-state ionization balance. Above $N_e = 10^{16}$ cm^{-3} collisional depopulation of the upper level of the strongly radiating transitions in O^{3+}–O^{5+} becomes comparable to radiative decay, and the radiative-power-loss coefficient drops nearly linearly with density. The behavior of L_z with electron density can be approximated by the expression

$$L_z = \frac{P_{\text{rad}}}{N_{\text{tot}} N_e} = \sum_i \sum_j C_i \frac{S_{ij}}{1 + \dfrac{N_e S_{ji}}{A_{ji}}} \Delta E_{ij} \ . \tag{5}$$

Here P_{rad} is the radiated power, N_{tot} is the total oxygen density, and C_i is the steady-state fractional abundance of charge state i. S_{ij} is the collisional excitation rate from the ground state of charge state i to the jth excited level, and ΔE_{ij} and A_{ji} are the energy separation of levels i and j and the radiative decay rate of the j-i transition, respectively.

The open and solid circles in Figs. 3 and 4 are the results obtained from the full model. They exhibit small

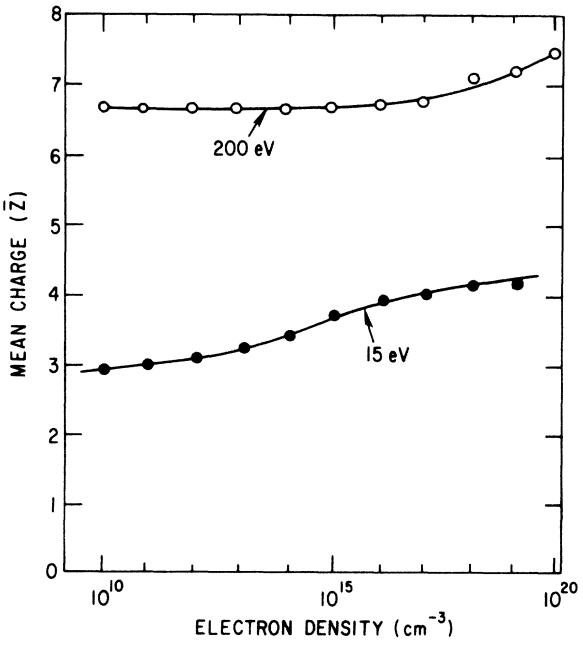

FIG. 4. Mean charge $\bar{Z}$ at electron temperatures of 15 and 200 eV plotted as a function of electron densiy; $\bar{Z}=1$ refers to O^{1+}.

variations from the sketched curves due to the fact that the temperature of the peak K- and L-shell emission shifts slightly due to changes in the ionization balance as the density is increased.

An alternative way of examining the radiated power coefficient for oxygen is in terms of the effective $\Delta E/kT_e$, where ΔE is the energy of a resonance transition in a plasma ion. In a companion paper[39] Skinner and Keane have derived an analytic model that yields an estimate of the optimum energy-level spacing $(\Delta E/kT_e)_{\text{opt}}$ that maximizes the radiative power loss at a given electron density and temperature.

At this point it should be emphasized that the steady-state radiative-power-loss coefficient as defined here and by other authors is an implicit function of the steady-state ionization balance. In the next section we describe generalized power-loss coefficients, appropriate for both steady-state and transient plasmas, that are ionization balance independent. In transient systems these generalized coefficients may be used to calculate the instantaneous total radiated power and net electron-energy-loss rate, while in the limit of steady-state ionization balance these coefficients yield the power-loss coefficient L_z.

IV. GENERAL CASE: IONIZING-RECOMBINING PLASMAS

The energetics of ionizing and recombining plasmas are of interest for a wide variety of plasmas, from the low-density plasmas employed in magnetic fusion research to the high-density laser-produced plasmas utilized in inertial confinement and soft-x-ray laser experiments. In particular, for x-ray laser schemes based on recombination of highly ionized ions, the total radiated power and net electron cooling rate are important, since these schemes rely on a rapid decrease of the electron temperature in a dense plasma to generate population inversion through fast three-body recombination and cascading to lower levels. Heat return to the electrons occurring during this process is a concern here since it may limit the decrease in electron temperature[40] and reduce the achievable population inversion. Since the collisional-radiative recombination rate scales approximately[41] as $T_e^{-9/2}$ when three-body recombination is dominant, attaining a low electron temperature is crucial to the success of recombination laser schemes.

In steady-state plasmas where the total radiated power is dominated by line emission, the dominant effect of radiation loss is to cool the electrons. In a transient plasma, however, the radiated power reflects potential energy changes due to ionization and recombination as well as electron energy losses occurring through collisional excitation. (During strong three-body recombination, potential energy changes may also result in electron heating.) The instantaneous radiated power depends on the current electron temperature and ionization balance; these in turn depend on the previous evolution of the electron temperature. For this reason, most calculations of radiation from transient plasmas to date have been for a specific electron temperature evolution, with limited applicability to ionizing and recombining plasmas in general.

In this section we define power-loss coefficients for transient plasmas that do not depend on an assumed temporal profile of the electron temperature. These coefficients can be used to determine the total radiated power (from both electron excitation and recombination contributions) and net electron cooling in a transiently ionizing or recombining plasma.

Consider two adjacent charge states of a given element, of charge z and $z+1$ and ground-state density N_z and N_{z+1}, respectively (see Fig. 5). We can write Eq. (3) for the excited-state populations $N_{i,z}$ of the ion of charge z in the following form:

$$\mathbf{N}_{i,z}=\mathbf{N}'_{i,z}+\mathbf{N}''_{i,z}\,, \tag{6}$$

$$\mathbf{N}'_{i,z}=-N_z\overleftrightarrow{\mathbf{Q}}^{-1}\cdot\mathbf{S}_{1,i}\,, \tag{7}$$

$$\mathbf{N}''_{i,z}=-N_{z+1}\overleftrightarrow{\mathbf{Q}}^{-1}\cdot\mathbf{R}_i\,. \tag{8}$$

Here $\mathbf{N}'_{i,z}$ is the fractional population of the excited states $\mathbf{N}_{i,z}$ arising from excitation of the ground state N_z $(=N_{1,z})$ while $\mathbf{N}''_{i,z}$ is the fraction arising from recombination of the ions N_{z+1} to N_z. (See Fig. 5.) In the steady-state situation, for transitions of importance to the total radiated power, it is generally the case that $\mathbf{N}_{i,z}\sim\mathbf{N}'_{i,z}$.

With the excited-state populations calculated as above we then define radiative power coefficients P for each charge state as follows:

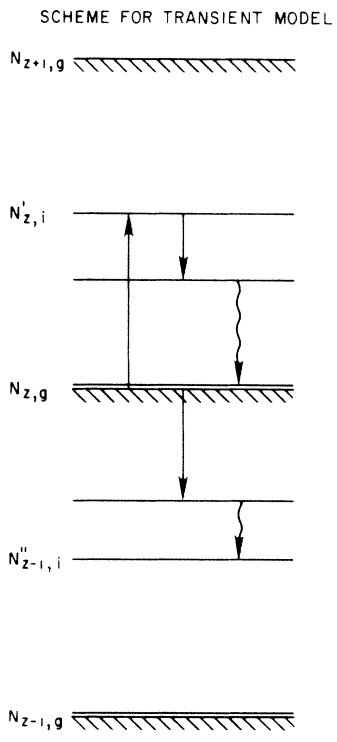

FIG. 5. Simplified energy-level diagram illustrating K and P coefficients defined in text. The arrows represent radiative and collisional processes generally.

$$P'_z = \sum_{i=2}^{k_{\max}} \sum_{j=1}^{i-1} (N'_{i,z} A_{ji} \Delta E_{ij}) / N_e N_z , \tag{9}$$

$$P''_z = \sum_{i=2}^{k_{\max}} \sum_{j=1}^{i-1} [N''_{i,z-1} A_{ji} \Delta E_{ij} + N_z N_e f_R(T_e) + N_z N_e f_B(T_e)] / N_e N_z . \tag{10}$$

In the above equations $k_{\max}$ is the total number of excited levels considered for the ion N_z, A_{ji} is the radiative decay rate between levels i and j, and ΔE_{ij} is the energy difference between levels i and j. P'_z and P''_z represent the radiated power per electron per ground ion N_z arising from collisional excitation of N_z and recombination of the ion N_z to N_{z-1}, respectively. Note that P''_z refers to line radiation in the ion of charge $z-1$ due to the recombination of ion z. Radiative recombination continua $[f_C(T_e)]$ and bremsstrahlung $[f_B(T_e)]$ are included in P''_z.

The net electron cooling or heating rate is also of interest, particularly for recombination x-ray laser studies. We define the electron cooling coefficients K'_z and K''_z as follows, with $N_{i,z-1}$ calculated as in Eq. (3):

$$K'_z = \lim_{N_{z+1} \to 0} \left[\sum_{i=1}^{k_{\max}-1} \sum_{j=i+1}^{k_{\max}} (N'_{i,z} S_{ij} - N'_{j,z} S_{ji}) N_e \Delta E_{ji} + \sum_{i=1}^{k_{\max}} (N'_{i,z} S_i N_e - N_{z+1} N_e^2 \beta_i) \chi_i \right] \Big/ N_e N_z , \tag{11}$$

$$K''_z = \lim_{N_{1,z-1} \to 0} \left[\sum_{i=1}^{k_{\max}-1} \sum_{j=i+1}^{k_{\max}} (N''_{i,z-1} S_{ij} - N''_{i,z-1} S_{ji}) N_e \Delta E_{ij} + \sum_{i=2}^{k_{\max}} (N''_{i,z-1} N_e S_i - N_z N_e^2 \beta_i) \chi_i \right] \Big/ N_e N_z . \tag{12}$$

Here S_i and β_i are the collisional ionization rate from level i and three-body recombination rate to level i, respectively, and χ_i is the ionization potential of level i. K'_z and K''_z represent the net electron cooling or heating arising from collisional excitation and ionization of N_z and recombination of N_z to N_{z-1}, respectively. The K''_z term is small in the steady-state case; however, in recombining high-density plasmas, the net electron heating due to three-body recombination as represented by K''_z can become large. The K and P coefficients defined here are similar in spirit to the P_0 and P_1 coefficients of McWhirter and Hearn,[42] although in this work the distinction between radiated power and electron cooling was not discussed.

The K and P coefficients for O^{4+}–O^{7+} for $N_e = 10^{14}$, 10^{16}, and 10^{18} cm^{-3} are shown in Figs. 6 and 7. The recombination coefficients for O^{8+} recombining to O^{7+} are also shown for $N_e = 10^{20}$ cm^{-3}. Each set of curves represents the excitation and recombination components of radiated power and electron cooling arising from the indicated ground state. The absolute value of the electron heating term K''_z is plotted since the scale is logarithmic (as defined K''_z is negative). There are four coefficients for O^{4+}, O^{5+}, O^{6+} and O^{7+}; for O^{8+} (bare nucleus) there is obviously no excitation-ionization contribution, and for O^{4+} only the P'_4 and K'_4 curves are shown, as the detailed model for O^{3+} required to compute the recombination curves P''_4 and K''_4 was not constructed.

A number of points may be made from these plots. As the electron density is increased, the K' and P' coefficients decrease due to the increasing importance of collisional deexcitation, which results in both a decrease in the radiated power and electron-energy-loss rate per electron per ion. At low temperatures, the recombination contributions as represented by K'' and P'' become larger than the excitation-ionization contributions. At lower densities the potential energy lost during recombination is emitted predominantly as photons; as the density is increased, however, electron heating becomes significant. As an example, at $N_e = 10^{18}$ cm^{-3} and for temperatures near 10 eV, each recombination of O^{5+} to O^{4+} results in roughly equal amounts of radiated power and electron heating. The temperature T_e^* at which the K' and K'' curves cross (for a given electron density and ground state) is the point at which electron cooling due to collisional excitation and ionization equals the electron heating due to three-body recombination processes, resulting in no net electron energy loss or gain. For $T_e > T_e^*$, collisional excitation and ionization processes result in net electron cooling; for $T_e < T_e^*$, the electrons are heated in the recombination of N_z to N_{z-1}.

These coefficients have the practical significance that it is possible to obtain the instantaneous radiated power and net electron cooling for an ionizing or recombining plasma from the electron temperature, density, and ground-state populations alone. The ground-state populations may be obtained by straightforward integration of Eqs. (2). This is a considerable simplification from a time-dependent calculation of the radiated power for a particular electron temperature evolution, and as such these coefficients are suitable for use in hydrodynamic codes to model atomic physics effects on the evolution of the electron temperature.

More specifically, for an element of atomic number Z present in a plasma with electron density N_e and electron temperature T_e in an arbitrary (equilibrium or nonequilibrium) state of ionization, the total instantaneous radiated power and electron cooling rates are

$$P_{\text{tot}} = N_e \sum_{i=0}^{Z} (N_i P'_i + N_{i+1} P''_{i+1}) , \tag{13}$$

$$K_{\text{tot}} = N_e \sum_{i=0}^{Z} (N_i K'_i + N_{i+1} K''_{i+1}) . \tag{14}$$

Here N_i and N_{i+1} are the ground-state populations of the ions of charge i and $i+1$. Thus, for an arbitrary temporal profile of T_e and ionization balance, calculation of the above sums gives the total radiated power and electron cooling. The detailed atomic physics involving level structure and rate coefficients is incorporated into the K and P coefficients.

The K and P coefficients are independent of the ionization balance. In fact, the steady-state radiative-power-loss coefficient L_z can be written as a linear sum of the P

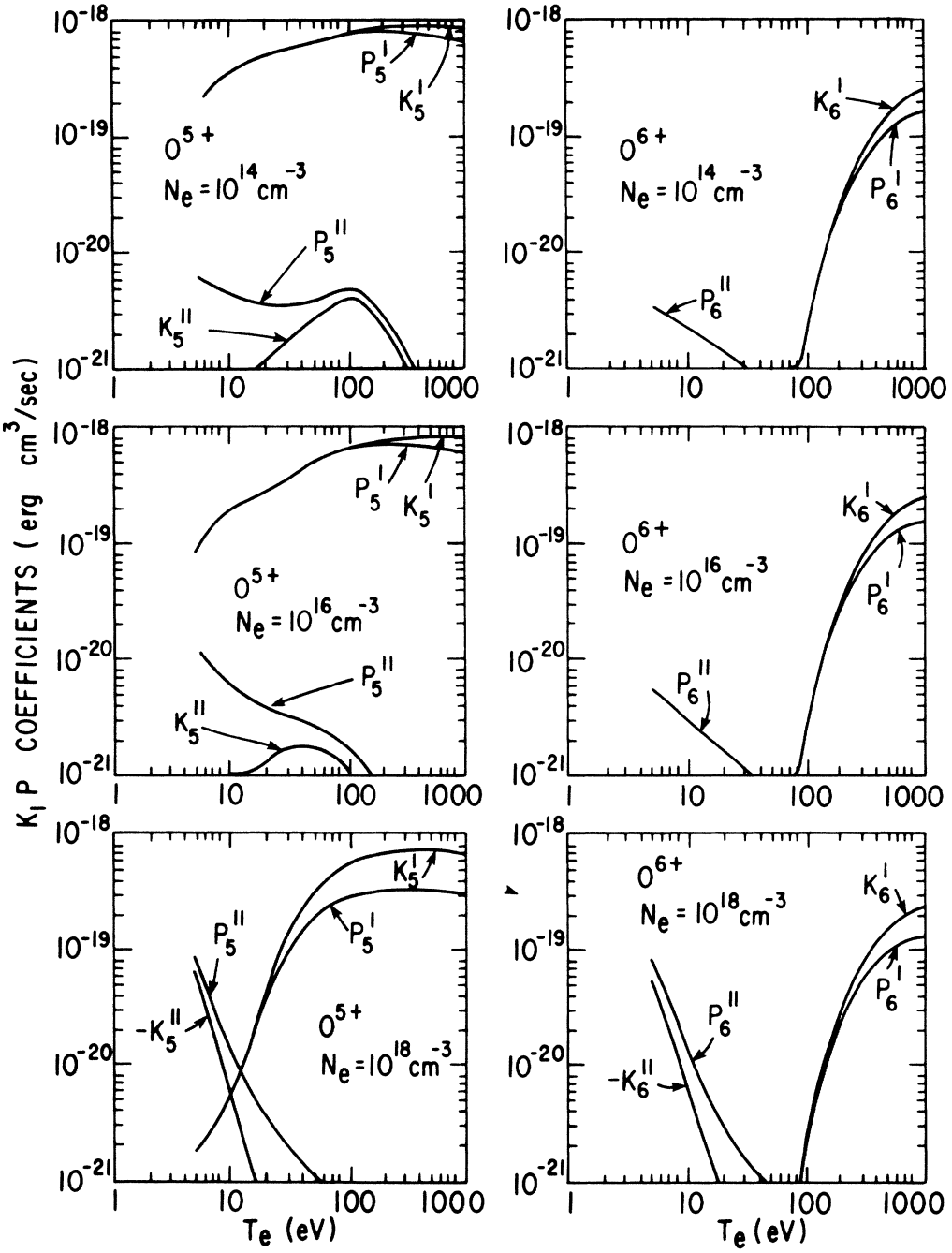

FIG. 6. Transient electron cooling and radiation loss coefficients K_z, P_z per ground-state ion per electron for O^{5+} and O^{6+}, as defined in text. In some cases K'' is too small to appear on the graph.

coefficients,weighted by the fractional abundances of each charge state:

$$L_z = \sum_{i=0}^{Z} (C_i P_i' + C_{i+1} P_{i+1}'') \ . \tag{15}$$

Here C_i is the steady-state fractional abundance of charge state i. The quantities C_i, P_i, and L_z are functions of N_e and T_e. In the low-density limit they are functions of T_e only, and the second term, which represents recombination contributions and bremsstrahlung, is generally small. It can also be shown form energy conservation that the K and P coefficients are related to the collisional dielectronic ionization and recombination coefficients S_{CR} and α_{CR} as follows:

$$K_z' = S_{CR} \chi_z + P_z' , \tag{16}$$

$$-K_z'' = \alpha_{CR} \chi_{z-1} - P_z'' \ . \tag{17}$$

Here χ_z is the ionization potential of the ion of charge z.

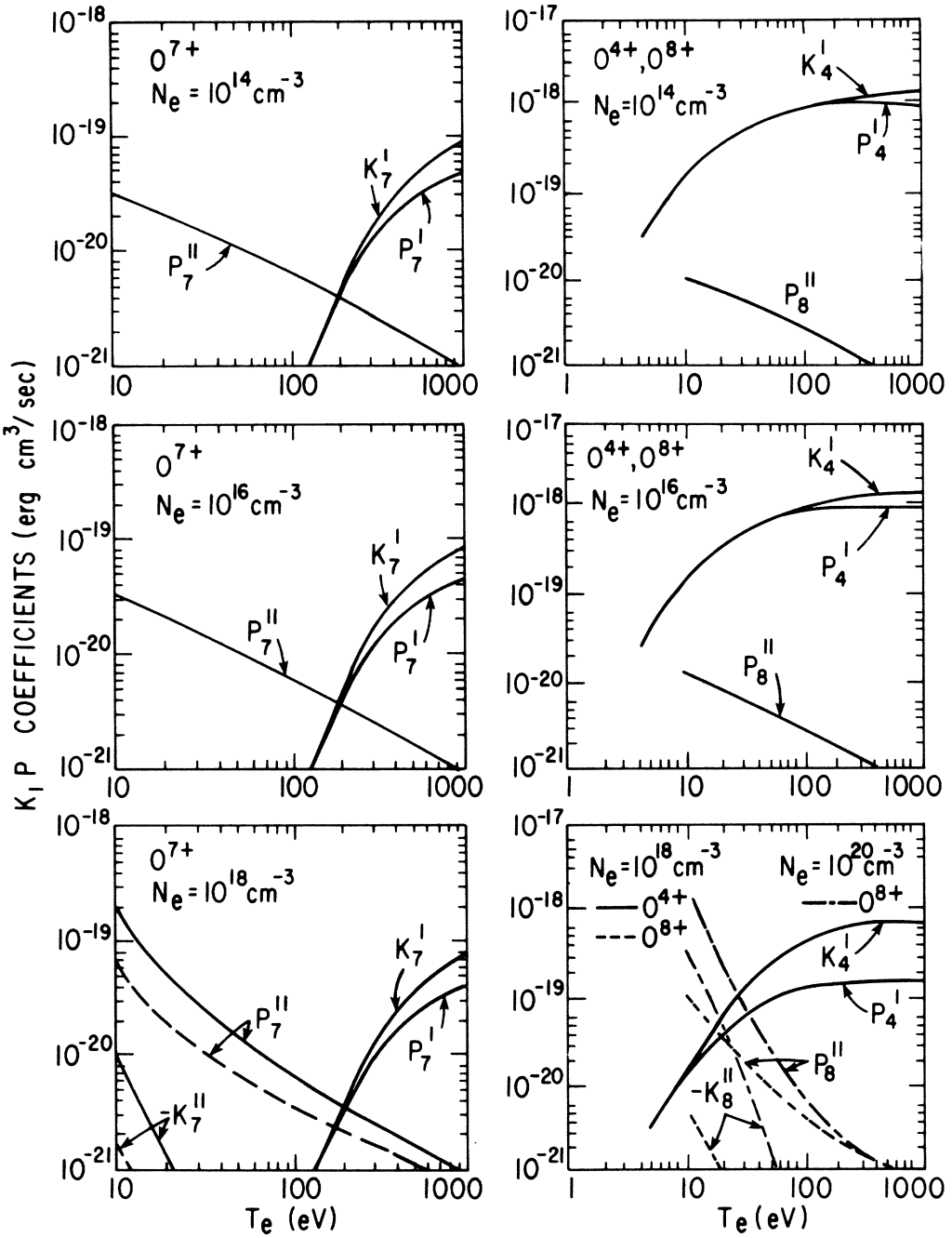

FIG. 7. Transient electron cooling and radiation loss coefficients K_z, P_z for O^{7+}, O^{8+}, and O^{4+} as defined in text. The dashed curves for O^{7+} at $N_e = 10^{18}$ cm^{-3} are from a calculation which did not take account of the metastable triplet levels in O^{6+}. The case for O^{8+} at $N_e = 10^{20}$ cm^{-3} (chain dashed) is included with O^{8+} at $N_e = 10^{18}$ cm^{-3} (dashed).

In the case of the excitation-ionization coefficients P_z' and K_z', the electron energy goes into direct ionization or collisional excitation followed by radiation or stepwise ionization. In Figs. 6 and 7 the difference between the P_z' and K_z' curves represents the electron energy going into collisional ionization. Note that $K_z' \sim P_z'$, for electron temperatures where, in steady state, charge state z is most abundant. As T_e increases, the K_z' and P_z' coefficients increase. This demonstrates that in a transient, ionizing plasma power losses at a given T_e are generally considerably greater than in the steady-state case. In the case of the recombination coefficients P_z'' and K_z'', Figs. 6 and 7 show that the ion potential energy is lost by photon emission and electron heating. The sum of the $-K_z''$ and P_z'' curves represents the ion potential energy loss due to recombination of charge state z to $z-1$.

We have investigated the effect of the inclusion of metastable levels in the calculation of the K and P coeffi-

cients. Figure 6 shows the K and P coefficients calculated for recombination of O^{7+} and excitation of O^{6+} with and without the triplet spin system of O^{6+}. Note the significant effect of the triplet spin system on the K_7'' and P_7'' coefficients. This is primarily due to the $2s\,^3S-2p\,^3P$ channel being available for electron excitation when the triplet system is included. The effect of the triplet spin system on the K_7' and P_7' coefficients is smaller, since, in general, excitation from the ground to the $2p\,^1P$ level is dominant over excitation to the $2s\,^3S$ and $2p\,^3P$ levels. Similar effects are observed for O V, although the differences between the singlet alone and singlet-triplet cases are not so large. Another effect of the triplet spin system is also apparent in Fig. 5; for O^{5+} at $N_e=10^{14}$ and 10^{16} cm^{-3}, the K_5'' curve is actually positive and represents electron cooling due to excitation of the $2s\,2p\,^3P\rightarrow 2p^2\,^3P$ and $2s\,2p\,^3P\rightarrow 2s\,3d\,^3D$ transitions. This demonstrates the importance of including the triplet spin system in radiative-power-loss calculations in dense transient plasmas, particularly in the recombining case.

Finally, a check of the atomic model can be performed using the K and P coefficients. This check involves comparing our results for the K and P coefficients to the ionization and recombination coefficients of Summers through Eqs. (16) and (17). Note that these equations can be rewritten as

$$S_{CR}X_z=K_z'-P_z', \tag{18}$$

$$\alpha_{CR}X_{z-1}=P_z''-K_z'' . \tag{19}$$

By comparing the right-hand side of each of these equations (calculated for O^{4+}–O^{7+}) to Summer's tabulated rates α_{CR} and S_{CR}, a consistency check of our excited-state model can be performed. The K and P coefficients relevant to H-like oxygen (K_7', P_7', K_8'', P_8'') show good agreement with Summer's rates, with the right-hand sides of (18) and (19) differing by at most 40% from the left-hand sides. For O V–O VII the agreement is within 30% for the K' and P' coefficients and a factor of 2.5 for the K'' and P'' coefficients when only the singlet spin system is considered for O V and O VII. Inclusion of the triplet spin system in P_5'',K_5'', and P_7'',K_7'' results in a difference of up to a factor of 4 between the two sides of (19), although in this case the comparison is not strictly valid, since Summer's rates do not include the effects of the triplet spin system. This comparison as well as the results discussed in the previous paragraph indicate that a significant advance would be realized if separate collisional-radiative dielectronic ionization and recombination coefficients for the singlet and triplet spin systems of O^{4+} and O^{6+} were available.[11]

V. APPLICATION TO TRANSIENT PLASMAS

In this section we apply the previous results to two situations. One case is a step-function rise of electron temperature T_e with time, such as may be experienced by a cold impurity ion entering a dense plasma; and the second is a specific electron temperature time evolution relevant to the laser-produced plasmas used in soft-x-ray laser experiments.

The case of an ionizing *coronal* plasma has been addressed by Carolan[14] who treated a step-function electron temperature rise and parametrized the cooling rate in terms of $N_e\tau_{SS}$ where τ_{SS} is the steady-state time, i.e., the time required for both the mean ionic charge and the cooling rate to reach 99% of the coronal equilibrium value. In the coronal limit the quantities L_z and $N_e\tau_{SS}$ are functions of temperature only; in the collisional-radiative regime this is no longer true. Figure 8 shows a plot of the oxygen steady-state time τ_{SS} versus electron temperature for $N_e=10^{10}$ and 10^{18} cm^{-3}. The peaks characterize the longer times required to ionize closed-shell configurations. The time required to reach equilibrium is governed by both the ionization and recombination rates. For $T_e>20$ eV the major change at high densities is the increase in the collisional-radiative ionization coefficient due to stepwise processes, and as a result $N_e\tau_{SS}$ is shorter at $N_e=10^{18}$ cm^{-3} than at $N_e=10^{10}$ cm^{-3}. For $T_e<20$ eV the reverse is true; the collisional interruption of dielectronic recombination results in a reduction in the recombination rate that outweighs the increased ionization rate, and hence there is a slower approach to equilibrium.

The effect on the radiated power is shown in Fig. 9, which shows the radiated-power-loss function L_z at several times for $N_e=10^{10}$ and 10^{18} cm^{-3}. The increase in radiated power in an ionizing plasma compared to an equilibrium plasma at the same temperature depends on the electron density and also, as in the coronal case,[14] is a strong function of whether the equilibrium charge state is of closed- or open-shell configuration. For example, in the broad region around 100 eV where He-like O^{6+} is dominant, the ionization rate from O^{5+} to O^{6+} is relatively high and thus equilibrium values of $\bar{Z}$ and L_z are gained more rapidly, particularly at high densities.

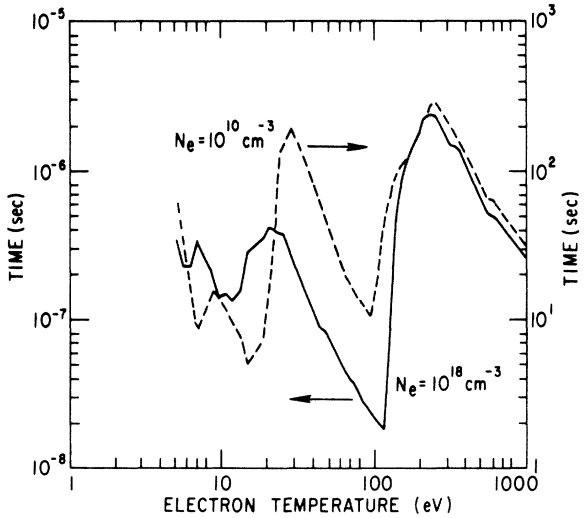

FIG. 8. Time required for both the radiation loss coefficient L_z and mean charge $\bar{Z}$ to be within 1% of their steady-state values for $N_e=10^{18}$ cm^{-3}, solid curve, time scale on left; and $N_e=10^{10}$ cm^{-3}, dashed curve, time scale on right.

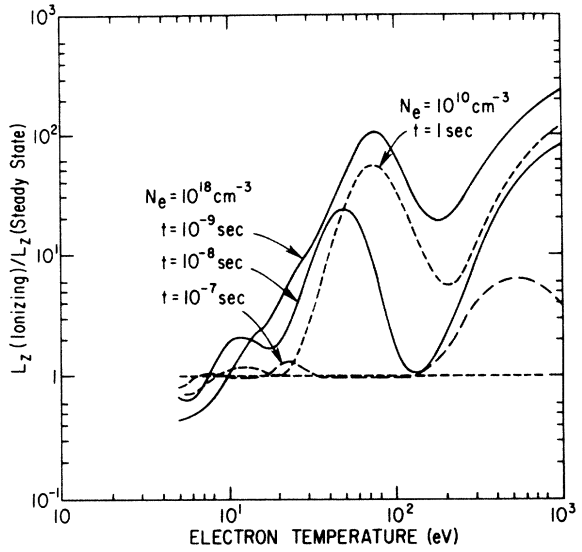

FIG. 9. Ratio of radiation loss coefficient at a given time after a step-function rise in electron temperature to its steady-state value. The dashed curve for $N_e = 10^{10}$ cm^{-3}, $t = 1$ sec is shown for comparison to the $N_e = 10^{18}$, $t = 10^{-8}$ sec case. The difference between these two curves represents the deviation from the coronal case where L_z(ionizing)/L_z(steady state) is a constant for a given $N_e t$.

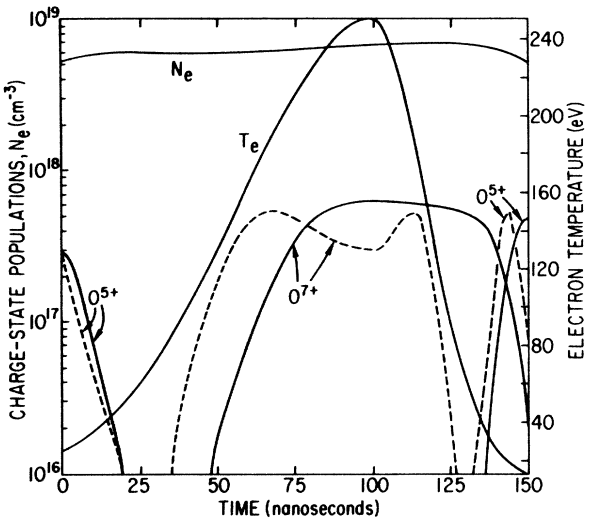

FIG. 10. Time evolution of oxygen ionization balance, T_e, and N_e for the electron temperature profile shown. The steady-state values of the O^{5+} and O^{7+} populations are indicated with dashed lines.

In the PPPL soft-x-ray laser development experiment,[1] a 1-kJ CO_2 laser pulse of 75 ns duration creates a carbon plasma composed primarily of hydrogenlike and totally stripped ions which are confined in a 90-kG magnetic field. Fast recombination produces a population inversion and gain on the C^{5+} 182-Å $n = 3 \rightarrow n = 2$ transition.

Figure 10 shows a typical electron temperature and electron density time history derived from a separate computer code used to simulate these magnetically confined, radiatively cooled plasmas. The carbon plasma has been seeded with aluminum in this case to increase the radiative cooling rate. This electron temperature time history was input to the present oxygen code as a first illustration of the energetics of oxygen radiation cooling and to demonstrate the use of the K and P coefficients. An oxygen density of 10^{18} cm^{-3} was assumed. Figure 10 also shows the time evolution of the O^{5+} and O^{7+} charge states and, for comparison, their steady-state values: it can be seen that transient effects are important in the computation of the ionization balance.

With the ionization balance computed, at each point in time the sums defined by Eqs. (13) and (14) were calculated. Figure 11 shows the temporal evolution of the radiated power, electron cooling, and the steady-state value of the radiated power at each point in time. In the transient case the electron-energy-loss rate exceeds the radiative power rate during the ionization phase, with the difference going into collisional ionization. During the phase of strongest recombination, near $t = 140$ ns, the radiated power is roughly twice its steady-state value. This additional radiation is mostly due to a loss of ion potential energy. The electron-energy-loss rate at this time is reduced from its steady-state value by a factor of 2.5 due to the electron temperature lagging behind the ionization balance (making the resonance transitions in O^{6+} and O^{7+} more difficult to excite) and also because of heat return to the electrons occurring primarily during recombination of O^{6+} to O^{5+}. At $t = 150$ ns, the electron cooling rate has become slightly negative due to heat return.

In an experiment the heat return during three-body recombination may be offset by adding additional cooling

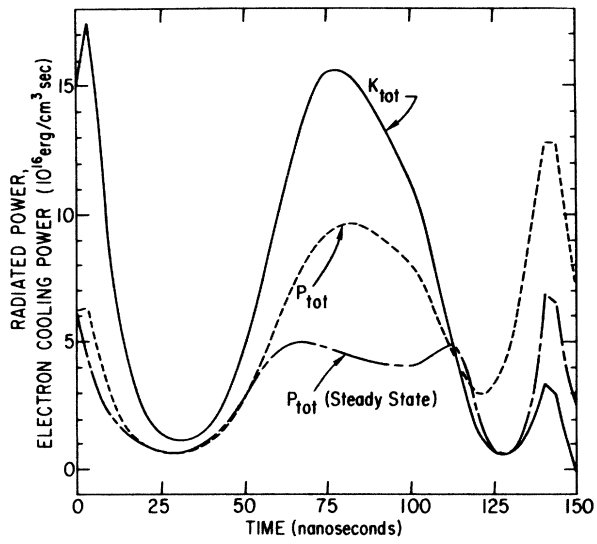

FIG. 11. Evolution of total radiated power, P_{tot}, and the net electron cooling power, K_{tot}, for the T_e profile in Fig. 10. The steady-state value of the total radiated power P_{tot} (steady state) is also shown.

elements to the plasma. The impurity elements chosen should have an ion abundance and energy-level structure as close as possible to the optimum for most effective radiation cooling of the electrons. A simple model[39] to evaluate different coolant ions for the maximum cooling at a given electron density and temperature will be reported separately. For the transient case shown here the electron cooling power has dropped at $t=130$ ns since the average $\Delta E/kT_e$ is about 20 due to the preponderance of He-like O^{6+} in the plasma. The predicted optimum $\Delta E/kT$ is about 1.5 for these conditions.

The general picture that arises in Figs. 10 and 11 is of radiation and electron cooling enhanced over the steady-state values during the ionization phase. During the recombination phase the radiation again exceeds its steady-state value, but the electron cooling rate is reduced. In a more complete simulation one would compute the electron temperature evolution self-consistently with the input energy source (laser heating, for example), the evolution of the ionization balance, and also any hydrodynamic motion. Such self-consistent calculations of the electron temperature evolution utilizing the K and P coefficients are underway and will be discussed in future work. This example, however, demonstrates the utility of the K and P coefficients in elucidating the kinetics in transient plasmas.

VI. CONCLUSIONS

We have calculated radiative-power-loss and electron cooling coefficients for oxygen in plasmas without invoking an assumption of coronal equilibrium. The discussion has primarily focused on the effects of increasing electron density and nonequilibrium ionization balance, which are the two factors that lead to the greatest departure from the coronal equilibrium power-loss rates. The results are thus applicable to the dense ($N_e \sim 10^{16}$–10^{20} cm^{-3}) transient plasmas typically produced in Z-pinch and laser-produced plasma experiments.

The results may be grouped into two classes, depending on whether the oxygen ionization balance has reached its steady-state distribution for the local value of electron temperature and density. In the case of steady-state ionization balance, the radiative-power-loss coefficient was found to be reduced from the coronal value as the electron density is increased due to the onset of collisional deexcitation, as well as shifts in the equilibrium ionization balance. At high density $\Delta n=0$ transitions are not primarily responsible for the radiated power loss for temperatures below 50 eV, unlike the coronal case. This is the reason the radiation peak at 20 eV becomes smaller than the peak at 200 eV as the electron density is increased.

In the case of nonequilibrium ionization balance, generalized power-loss coefficients K and P were derived and discussed in detail. These coefficients are motivated by the fact that in transient plasmas, in contrast to equilibrium plasmas, the net electron-energy-loss rate may differ greatly from the radiated power rate. These coefficients are independent of the temporal evolution of the electron temperature and are suitable for use in modeling atomic physics effects on the electron temperature in dense transient plasmas. They enable the radiated power and net electron cooling rate to be calculated self-consistently with the instantaneous local ionization balance, electron temperature, and electron density. In addition, these coefficients determine the temperature T_e^* for a given charge state in strongly recombining dense plasmas at which electron energy loss through collisional excitation and ionization is balanced by electron heating occurring due to three-body recombination. Finally, the results for the recombination contributions K'' and P'' were found to be quite sensitive to the inclusion of the triplet spin system (for O^{4+} and O^{6+}) indicating the need for inclusion of the triplet spin system in detailed calculations of radiated power.

The use of the K and P coefficients was demonstrated in two ways. First, the radiative loss properties and equilibration times for neutral oxygen exposed to a step-function increase in electron temperature were examined. The normalized time $N_e\tau_{SS}$ at $N_e=10^{18}$ cm^{-3} was found to decrease from its value at $N_e=10^{10}$ cm^{-3} for $T_e>20$ eV due to the increase in the collisional-radiative ionization coefficient with density. For $T_e<20$ eV a decrease in the collisional radiative recombination coefficient with density led to an increase in $N_e\tau_{SS}$ for $N_e=10^{18}$ cm^{-3}. Similar behavior was noted for the quantity L_z(ionizing)/L_z(steady state).

Secondly, an electron temperature profile derived from a separate simulation program was used to study the radiative cooling properties of oxygen in a transiently ionizing and recombining high-density plasma. During the ionization phase both the electron-energy-loss rate and the total radiation are increased over their steady-state values. During strong recombination, the radiated power still exceeds the corresponding steady-state value, but the electron cooling power is significantly less due to both the electron temperature lagging behind the ionization balance as well as electron heating during three-body recombination.

In future work we plan to extend this study to other elements and to examine the feasibility of utilizing radiation losses from high-Z ions as an effective electron coolant in dense transient plasmas. The methods described here have been used to model the evolution of the electron temperature in a carbon plasma seeded with aluminum, and these results will be reported in the near future. The formalism outlined in this paper should provide a framework for systematically examining the power-loss properties of a variety of elements suitable for electron cooling in recombination soft-x-ray laser experiments.

ACKNOWLEDGMENTS

We wish to thank S. Suckewer and R. A. Hulse for useful discussions. This work was supported by the U.S. Department of Energy (Office of Basic Energy Sciences) and the U.S. Air Force Office of Scientific Research, under Contract No. AFOSR-84-0025.

*Present address: Lawrence Livermore National Laboratory, University of California, Livermore, CA 94550.

[1]S. Suckewer, C. H. Skinner, H. Milchberg, C. Keane, and D. Voorhees, Phys. Rev. Lett. **55**, 1753 (1985), and references therein.

[2]D. L. Matthews, P. L. Hagelstein, M. D. Rosen, M. J. Eckart, N. M. Ceglio, A. U. Hazi, H. Medecki, B. J. MacGowan, J. E. Trebes, B. L. Whitten, E. M. Campbell, C. W. Hatcher, A. M. Hawryluk, R. L. Kaufmann, L. D. Pleasance, G. Rambach, J. H. Scofield, G. Stone, and T. A. Weaver, Phys. Rev. Lett. **54**, 110 (1985).

[3]M. D. Rosen, P. L. Hagelstein, D. L. Matthews, E. M. Campbell, A. U. Hazi, B. L. Whitten, B. J. MacGowan, R. E. Turner, R. W. Lee, G. Charatis, G. E. Busch, C. L. Shepard, and P. D. Rockett, Phys. Rev. Lett. **54**, 106 (1985).

[4]J. P. Apruzese, J. Davis, M. Blaha, P. C. Kepple, and V. L. Jacobs, Phys. Rev. Lett. **55**, 1877 (1985).

[5]J. F. Seely, C. M. Brown, U. Feldman, M. Richardson, B. Yaakobi, and W. E. Behring, Opt. Commun. **54**, 289 (1985).

[6]C. H. Nam, E. Valeo, S. Suckewer, and U. Feldman, Bull. Am. Phys. Soc. **30**, 1600 (1985).

[7]C. Breton, C. de Michelis, and M. Mattioli, J. Quant. Spectrosc. Radiat. Transfer **19**, 367 (1978).

[8]D. E. Post, R. V. Jensen, C. B. Tarter, W. H. Grassberger, and W. A. Lokke, At. Data Nucl. Data Tables **20**, 397 (1977).

[9]V. L. Jacobs, J. Davis, J. Rogerson, and M. Blaha, J. Quant. Spectrosc. Radiat. Transfer **19**, 591 (1978).

[10]H. P. Summers and R. W. P. McWhirter, J. Phys. B **12**, 2387 (1979).

[11]H. P. Summers and M. B. Hooper, Plasma Phys. **25**, 1311 (1983).

[12]D. Duchs, W. Englehardt, and W. Koppendorfer, Nucl. Fusion **14**, 73 (1974).

[13]J. Rogerson, J. Davis, and V. L. Jacobs, J. Quant. Spectrosc. Radiat. Transfer **19**, 217 (1978).

[14]P. G. Carolan and V. A. Piotrowicz, Plasma Phys. **25**, 1065 (1983).

[15]D. Duston and J. Davis, Phys. Rev. A **23**, 2602 (1981).

[16]D. Duston and J. Davis, J. Quant. Spectrosc. Radiat. Transfer **27**, 267 (1982).

[17]H. P. Summers, Mon. Not. R. Astron. Soc. **169**, 663 (1974); Appleton Laboratory Report No. IM367, 1974 (unpublished).

[18]H. P. Summers, Comments At. Mol. Phys. **14**, 147 (1984).

[19]D. R. Bates, A. E. Kingston, and R. W. P. McWhirter, Proc. R. Soc. London Ser. A **267**, 297 (1962).

[20]S. Suckewer, J. Phys. B **3**, 380 (1970).

[21]W. L. Wiese, M. W. Smith, and B. M. Glennon, *Atomic Transition Probabilities,* Natl. Bur. Stand. (U.S.), Natl. Stand. Ref. Data Ser. No. 4 (U.S. GPO, Washington, D.C., 1966), Vol. 1.

[22]S. Bashkin and J. Stoner, *Atomic Energy Levels and Grotrian Diagrams* (North-Holland, Amsterdam, 1975), Vol. 1.

[23]P. S. Kelly, J. Quant. Spectrosc. Radiat. Transfer **4**, 117 (1964).

[24]D. R. Bates and Agnete Damgaard, Philos. Trans. R. Soc. London Ser. A **242**, 101 (1949).

[25]K. L. Bell, H. B. Gilbody, J. G. Hughes, A. E. Kingston, and F. J. Smith, Culham Laboratory (Abingdon) Report No. CLM-R216, 1982 (unpublished).

[26]L. Vriens and A. H. M. Smeets, Phys. Rev. A **22**, 940 (1980).

[27]R. H. Clark, D. H. Sampson, and S. J. Goett, Astrophys. J. Suppl. Ser. **49**, 545 (1982).

[28]D. H. Sampson and L. B. Golden, Astrophys. J. **170**, 169 (1971).

[29]A. K. Pradhan, D. W. Norcross, and D. G. Hummer, Astrophys. J. **246**, 1031 (1981).

[30]D. Cochrane and R. W. P. McWhirter, Phys. Scr. **28**, 25 (1983).

[31]Y. Itikawa, S. Hara, T. Kato, S. Nakazaki, M. Pirdzola, and D. Crandall, Institute of Plasma Physics, Nagoya, Japan, Report No. IPPT-AM-27, 1983 (unpublished).

[32]M. J. Seaton, in *Atomic and Molecular Processes,* edited by D. R. Bates (Academic, New York, 1962), p. 374.

[33]R. M. Pengelly and M. J Seaton, Mon. Not. R. Astron. Soc. **127**, 165 (1963).

[34]D. H. Sampson and A. D. Parks, Astrophys. J. Suppl. Ser. **28**, 323 (1974).

[35]T. Fujimoto, J. Quant. Spectrosc. Radiat. Transfer **21**, 439 (1979).

[36]M. J. Seaton, Mon. Not. R. Astron. Soc. **119**, 81 (1959).

[37]W. Karzas and R. Latter, Astrophys. J. Suppl. Ser. **6**, 167 (1961).

[38]W. Eisner and M. J. Seaton, J. Phys. B **7**, 2533 (1974).

[39]C. H. Skinner and C. Keane, Appl. Phys. Lett. (to be published).

[40]P. T. Rumsby and J. W. M. Paul, Plasma Phys. **16**, 247 (1974); M. Mattioli, Plasma Phys. **13**, 19 (1971).

[41]E. Hinnov and J. Hirschberg, Phys. Rev. **125**, 795 (1962).

[42]R. W. P. McWhirter and A. G. Hearn, Proc. Phys. Soc. London **82**, 641 (1963).